Annals of Agricultural & Crop Sciences

Open Access

Austin Publishing Group

Research Article

Crop Identification and Health Assessment Through Nanoscale Spectral Remote Sensing Inputs

Muhammad Usman Saeed[1]; Imdad Ullah[1]*; Saeed Ahmad[2]

[1]School of Economics, Bahauddin Zakariaya University, Multan, Pakistan

[2]Language Centre, University of Eastern Finland, Finland

***Corresponding author:** Imdad Ullah, School of Economics, Bahauddin Zakariaya University, Multan, Pakistan.

Email: muhammadusmansaeed66@gmail.com

Received: October 15, 2024; **Accepted:** November 04 2024; **Published:** November 11, 2024

Abstract

Food, textiles, fuel, and raw materials are produced through agriculture, all essential for human survival. At the same time as the human population is reaching previously unheard-of heights and continuing to grow, this function must be fulfilled in the current environment of environmental sustainability, climate change, and the continued viability of agricultural activities to provide for both subsistence and livelihoods. Remote sensing has the potential to support the adaptive evolution of agricultural methods to meet this significant challenge by consistently providing data on crop status throughout the growing season at various scales and for multiple actors. Significant improvements in capabilities, particularly the creation of spectral-temporal profile models, can be used for crop identification. As inputs to crop growth and yield models, the same model form can be used to estimate crop development stage, leaf area index, and canopy light interception. We have taken the data from six important crops and compared the spectral pattern and leaf properties to understand the rule and potential of nanoscale remote sensing to identify crop health at the growing stage. Understanding Crop breeding, monitoring agricultural land usage, predicting crop yields, and ecosystem services related to soil and water resources or biodiversity loss is crucial.

Keywords: Crops vegetation; Precision farming; Ecosystem services; Chlorophyll

Introduction

History has documented significant and irregular variations in crop output worldwide. Crop production has varied dramatically over the previous three decades, even as new, higher-yielding crop types and improved production techniques have been deployed. Effective crop production, processing, distribution, and marketing decisions depend on timely and precise crop production predictions and estimates [22,23]. Understanding agricultural conditions worldwide is particularly planting bed to a need for accurate, current information on global food supplies; decisions on plan-recurrent selling, storing, transporting, and buying must be made with partial information. However, only a few countries have adequate systems for obtaining and reporting crop production statistics; accesses vary significantly from country to country.

During the past few years, we have discovered that remote sensing from aeronautical platforms may deliver precise, fast data on crop output. Large-area crop surveys are made possible by the synoptic view of agricultural landscapes afforded by multispectral sensors on satellite platforms in conjunction with computer-aided analytical techniques [1]. The Large Area Crop Inventory Experiment (LACIE) amply proved the viability of using satellite-acquired multispectral data to identify and estimate the area of one crucial crop, wheat. Later, the USDA, NASA, and NOAA's AgRISTARS program later expanded the LACIE crop identification-area estimation methodology to accommodate other crops and locations [10,11].

All energy that travels in a harmonic wave pattern at the speed of light is known as Electromagnetic (EM) energy. A harmonic wave pattern comprises waves that happen at regular intervals. The EMR has both a wave model and a particle model. The wave model explains the propagation (movement) of EM energy. The interaction between this energy and the substance, however, is what allows for its detection. In this interaction, photons, which are numerous individual bodies/particles with such particle-like qualities as energy and momentum, behave like EM energy contain reviews on the nature of EM radiation and physical principles [9,11]. The EMS is a continuum of energy propagating through vacuums like space at the speed of light (3 × 108 ms-1), with wavelengths ranging from meters to nanometers. The EMS covers a wide range of wavelengths, from 10-10 µm (cosmic rays) to 1010 µm (radio waves) [21]. The EMS's ultraviolet, visible, infrared, and microwave sections have all been broadly classified. However, these distinctions were made at random. The boundary between one nominal spectral region and the next must be clarified. The region of the EMS where optical techniques of refraction and reflection can be utilized to focus and divert radiation is known as the visual wavelengths, which range from 0.30 to 15 µm. EM energy can be refracted and reflected by solid materials at these wavelengths. The reflective section of the spectrum is often defined as the range between 0.38 and 3.0 µm [12,33]. Most energy detected at these wavelengths is solar radiation reflected off Earthly objects.

Citation: Saeed MU, Ullah I, Ahmad S. Crop Identification and Health Assessment Through Nanoscale Spectral Remote Sensing Inputs. Ann Agric Crop Sci. 2024; 9(5): 1168.

The term "ultraviolet," which refers to an area of short-wavelength radiation between the X-ray zone and the visible range (0.40 to 0.70 μm) of the EMS, literally means "beyond violet." The near ultraviolet (0.32 to 0.40 μm), the far ultraviolet (0.32 to 0.28 μm), and the extreme ultraviolet (below 0.28 μm) are three standard divisions of the ultraviolet region. These divisions are often called UV-A, UA-B, and UA-C, respectively [24].

The Near-Infrared (NIR) ranges in wavelength from 0.72 to 1.30 μm, the middle infrared/shortwave infrared ranges from 1.30 to 3 μm, and the far infrared ranges from 7.0 to 15.0 μm. The infrared region spans from 0.72 to 15 μm and has been split into these three main divisions. The behavior of radiation in the NIR range is similar to that in the visible spectrum. As a result, films, filters, and cameras made for visible light can also be used for remote sensing in the NIR [21,38]. The far-infrared region (7.0 to 15 μm) includes wavelengths that go well beyond the visible spectrum and extend into areas next to the microwave spectrum. The Earth mainly emits far-infrared radiation. No particular name typically refers to the range of wavelengths from 3.0 to 7.0 μm [35].

The microwave spectrum spans a distance of 1mm to 1m. The longest wavelengths frequently employed in remote sensing are microwaves. The thermal energy of the far-infrared region shares many characteristics with the shortest wavelengths in this range. It is further separated into various frequency bands frequently employed in remote sensing (1 GHz = 10^9Hz). In contrast to the optical portion of EMS, where spectral bands are defined by wavelength, the microwave region of EMS often uses frequencies to do so [3-5]. About 4% of all solar radiation entering the planet is reflected into space by the Earth's land surface. The atmosphere reflects the remaining energy or absorbs it and emits it as infrared radiation. The varied surface features of the Earth absorb and reflect radiation at various wavelengths in varying amounts. The spectral response pattern of an object refers to the amount of energy it emits or reflects throughout a broad range of wavelengths [12,13]. These responses have frequently been referred to as spectral signatures because spectral responses obtained by distant sensors over a variety of features often allow an assessment of the type and condition of the features. Even though many Earth surface features exhibit distinctive spectrum reflectance and emittance characteristics, these traits produce spectral "response patterns" rather than spectral "signatures." The term signature tends to imply an absolute and singular pattern, which is why this is the case. The spectral patterns seen in the natural world do not work like this [9].

The spectral reflectance pattern of the main elements of the terrain, including the soils, plants, and shallow and deep water. Vegetation is highly noticeable in its ability to absorb incident light in the blue (400 to 500 nm), red (600 to 700 nm), and shortwave-infrared regions (at 1400, 1900, and 2600 nm) wavelength ranges (Bian et al. 2016). While chlorophyll, which gives plants their green color, is responsible for absorptions in the blue and red spectrum, water absorbs incident light in the shortwave-infrared range [8].

Contrary to vegetation, water reflects more in the blue region (400 to 500 nm) and absorbs most in the NIR area (700 to 1300 nm), according to this comparison of these two spectral response patterns. Notably, the NIR area is where vegetation reflects the most. Using air/space carried multispectral images, this contrasting feature enables vegetation recognition from water bodies [28]. On the other hand, soils, except for two absorption bands centered on 1400 and 1900 nm, have a rising trend in their spectral reflectance pattern with increasing wavelengths.

The word "hyper" in "hyperspectral" refers to the numerous measured wavelength bands and signifies "over" as in "too many." Because hyperspectral images are spectrally over determined, so they provide sufficient spectral information for identifying and distinguishing objects [4]. The word "hyper" in "hyperspectral" refers to the numerous measured wavelength bands and signifies "over" as in "too many." Because hyperspectral images are spectrally over determined, so they provide sufficient spectral information for identifying and distinguishing objects [1].

Every object, alive or inanimate, has a unique spectral signature encoded in the spectrum of the light it reflects or emits. The constituent substances' electronic and vibrational energy states govern the object's distinct spectrum properties [29]. Through various spectrum analysis techniques, these spectral features enable that object or importance to be recognized.

The strength of the measurements of the spectral response patterns in several contiguous, narrow spectral bands has been acknowledged. Landsat -TM's spectral bands are denoted by the numerals 1 through 7, and their bandwidths are shown in distinct blue lines. At seven locations between 350 and 2,500 nm, the spectral response of green vegetation has been combined and given a blue color [32,35]. Green is used consistently throughout to represent the hyperspectral response pattern of green vegetation. Green foliage has a constant spectral response pattern, except between 1,800 and 2,000 nm. Due to discontinuous and broad spectral bands, the thematic Mapper could not record the water absorption band at 1,400 nm and two absorption patterns in the near-infrared plateau at 1,000 nm and 1,200 nm. Similarly, it is possible to create spectra for different terrain features, such as soil, water, and plants.

The hyperspectral data are challenging to visualize simultaneously due to their several spectral bands. Making an image cube is one method of comprehending the patterns in the data because each ground scene can be composed of hundreds of images (bands). The spatial dimensions that display the terrain's ground surface are the x and y axes. All the other bands make up the z-axis as if they were piled like a ream of paper and turned on their side. The top image is a three-band composite created from three bands (often R, G, and B) for presentational purposes. The colors streaming away from the edges are the edge pixel values along the z-axis, which are rainbow-colored from blue to red [12,37]. This way, one can observe how the spectra vary and that a tremendous amount of information is stored in ranges by following an edge pixel in this cube along the z-axis.

Table 1: Commonly used microwave frequencies.

Band frequency (GHz)	Wavelength (cm)
P band: 0.3 – 1	30 – 100
L band: 1 – 2	15 – 30
S band: 2 – 4	7.5 – 15
C band: 4 – 8	3.8 – 7.5
X band: 8 – 12.5	2.4 – 3.8
Ku band: 12.5 – 18	1.7 – 2.4
K band: 18 – 26.5	1.1 – 1.7
Ka band: 26.5 – 40	0.75 – 1.1

A platform, instrumentation (sensor), data reception, processing, and analysis comprise a remote sensing system that measures, observes, and forecasts the Earth's system's physical, chemical, and biological elements. Our objective of this study is to identify the rule of the nanoscale spectral remote sensing inputs to monitor the health of the crop and compare the spectral signatures pattern and the leaf characteristics of the six different vegetables and cereal crops.

Material and Methods

Data

The optical characteristics of crop leaves can be measured through experimental processes, and deterministic methods based on various models of light interactions with crop leaves can also be created. The underlying physics and the leaf's complexity set these models apart [36]. The simplest ones treat the blade as a single scattering and absorbing layer. The structure, size, location, and molecular makeup of each cell have been defined in detail in the more complex ones. Whatever the method, these models have increased our comprehension of how light interacts with plant leaves. They can be divided into many classes and ordered according to increasing complexity. We collect the data for five crops from https://ecosis.org/package/leaf-optical-properties-experiment-database--lopex93-

Satellite-based remote sensing systems play a vital role in agricultural applications by providing a wide spatial coverage and a systematic acquisition of data. These systems consist of Earth-observing satellites equipped with various sensors designed to capture different spectral bands of the electromagnetic spectrum (Figure 1).

Agriculture plays a vital role in global food security and sustainable development. To ensure optimal crop production and resource management, accurate and timely information about crops is crucial. Agricultural remote sensing offers a non-intrusive means of acquiring valuable information about crops and their surrounding environment.

The Landsat program, initiated by NASA and the United States Geological Survey (USGS), has been a cornerstone in Earth observation since the launch of Landsat-1 in 1972. Currently, Landsat-8 and Landsat-9 are the operational satellites in this series. Landsat satellites capture imagery in several spectral bands, including visible, near-infrared, shortwave infrared, and thermal infrared. The spatial resolution of Landsat imagery is typically 30 meters, providing moderate detail for agricultural monitoring. Landsat satellites have a revisit time of approximately 16 days, allowing for regular monitoring of agricultural areas. The Landsat data archive, available to the public, provides a valuable resource for long-term analysis of land cover, crop health, and vegetation dynamics [18,34] .

The European Space Agency (ESA) operates the Sentinel series of satellites, which are part of the Copernicus program, an initiative aimed at providing open and free access to Earth observation data. Sentinel-2, in particular, is of great importance in agricultural remote sensing [34]. It consists of a constellation of satellites equipped with a multispectral imaging instrument that captures imagery in 13 spectral bands, ranging from the visible to the shortwave infrared region. Sentinel-2 has a higher spatial resolution than Landsat, with 10-meter and 20-meter bands, enabling detailed analysis of agricultural fields. Moreover, its revisit time is around 5 days, offering more frequent data acquisition, especially beneficial for time-critical agricultural activities like crop monitoring and disease detection [25,30].

Remote sensing data offer wide spatial coverage, moderate to high spatial resolution, and varying spectral bands, enabling the monitoring of crop health, land cover changes, and vegetation dynamics. The availability of open data from these systems has fostered research and innovation in agricultural remote sensing, contributing to improved decision-making and sustainable agricultural practices (Figure 2).

B. Methodology

Allen and Richardson [2] introduced the first plate model, which depicted a leaf as an absorbent plate with rough surfaces that led to Lambertian diffusion. Here, the variables are the absorption coefficient and the index of refraction. The reflectance spectrum of a small crop leaf with few air-cell wall contacts is accurately modeled by this model. By seeing non-compact leaves as collections of N plates separated by N-1 air spaces, the same authors quickly expanded the model to include them. Similar to the scattering coefficients in the Kubelka-Munk model, this extra parameter N describes the interior structure of the leaf. The prospecting model (Leaf Optical Properties Spectra), now widely used in remote sensing, was created in this manner [15]. The hemispherical reflectance and transmittance of different plant leaves (monocots, dicots, or senescent leaves) spanning the solar spectrum from 400 nm to 2500 nm were accurately simulated by this algorithm, which was among the first radiative transfer codes to do so. Several versions that have been validated on various datasets have been widely distributed in the community [14,15].

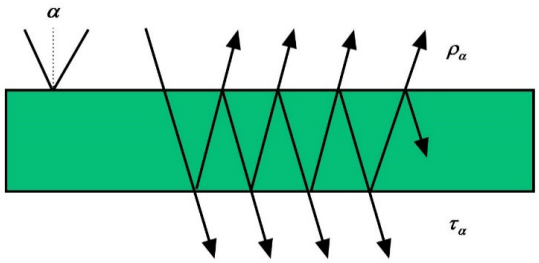

$$\rho_\alpha = [1 - t_{av}(\alpha, n)] + \frac{t_{av}(90,n)t_{av}(\alpha,n)\theta^2[n^2 - t_{av}(90,n)]}{n^4 - \theta^2[n^2 - t_{av}(90,n)]^2} \quad (1)$$

$$\tau_\alpha = \frac{t_{av}(90,n)t_{av}(\alpha,n)\theta n^2}{n^4 - \theta^2[n^2 - t_{av}(90,n)]^2} \quad (2)$$

Where,

α = maximum incidence angle defining the solid angle Ω

n = refractive index

t_{av} = transmittance

θ = transmission coefficient of the plate

$t_{av}(\alpha, n)$ = is the transmissivity of a dielectric plane surface

Results and Discussion

Optical Properties of Aample Crops Leaves

Most incident radiation passes through the leaf and interacts with its interior structure and parts. Three zones, each linked with

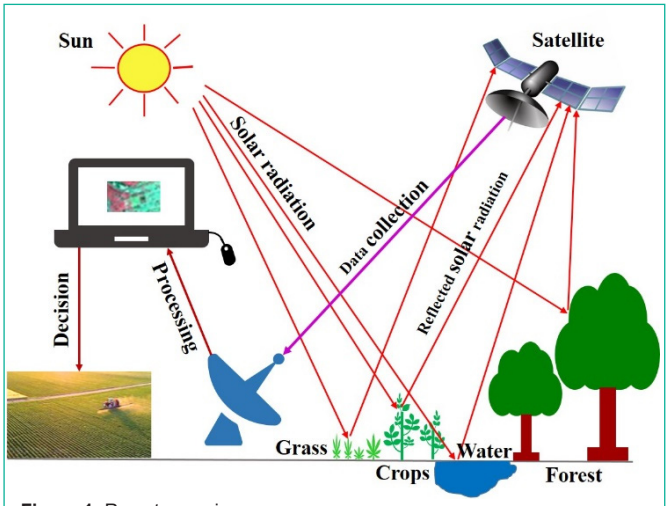

Figure 1: Remote sensing processes.

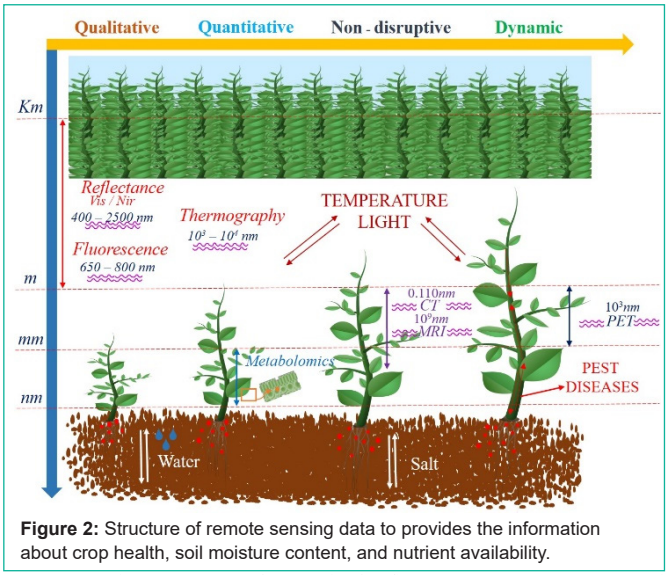

Figure 2: Structure of remote sensing data to provides the information about crop health, soil moisture content, and nutrient availability.

a separate phenomenon affecting leaf reflectance, transmittance, and absorption, have been identified in the 400 to 2500 nm wavelength range. The reflectance of leaves is relatively low in the visible part of the spectrum due to leaf absorption, which results in low reflectance (and transmittance). But there is a noticeable increase in reflectance in the near-infrared spectrum. In general, leaves reflect 40 to 50 percent of incident energy at these wavelengths and absorb less than 5 percent [19,35]. The many reflections in the internal mesophyll structure, which are brought on by the variations in the refractive indices of the cell walls and intercellular air cavities, account for the high reflectance as well as transmittance in the near-infrared "plateau" between 800 and 1400 nm. Reflectance differences are usually more extensive in the near-infrared than in the visible wavelengths because interior leaf structure differs significantly among species. The near-infrared reflectance of leaf layers increases due to repeated transmittance and reflectance (Figure 3), reaching its maximum or infinite reflectance at roughly eight leaf layers, or 70 to 80 percent. The reflectance of green vegetation in the middle-infrared region (1400-2500 nm) of the spectrum is dominated by large water absorption bands that occur near 1400, 1900 and 2500 nm; however, the water content of leaves also has a significant impact on the areas in between these absorption bands. An equivalent water thickness can be absorbed to simulate the spectral absorption characteristics in this region, where leaf reflectance is inversely related to the total amount of water in the leaf [16,31].

Reflectance, transmittance, and absorption by leaves depend on the concentration of pigments and water and the internal cell structure of each species. The type of leaf, stage of development, senescence, and stress all affect these physiological and morphological quantities. Regarding leaf type, there are notable differences between the reflectance properties of dicotyledon leaves with dorsiventral mesophylls and monocotyledon leaves with undifferentiated mesophyll, particularly in the near-infrared region [17]. When leaves grow and mature, their visible reflectance decreases, and their near-infrared reflectance increases. The mesophyll in adult leaves has more significant intercellular air gaps than the more compact immature leaves, which is thought to be the cause of this phenomenon [20]. In contrast to maturation, senescence causes visible reflectance to increase due to chlorophyll loss and infrared reflectance to decrease, though relatively less so than the increase in visible reflectance.

Numerous stresses, including nutrient deficiencies, salt, water deficits, and insect and disease damage, also influence plant leaves' optical properties. These stresses are typically accompanied by reduced chlorophyll production, causing increased reflectance in the visible region. In the infrared, reflectance is usually lowered by these types of strains, while stress producing a loss of water results in enhanced infrared reflectivity. However, alterations in reflectance become noticeable once the leaves are almost 75% turgid [12,36].

Phisical Properties of Sample Crops Leaves: One of the most crucial components of a plant is the leaf. The size, shape, thickness, mass, and color of leaves on various plants vary greatly. Inside all leaves are substances called pigments, which give leaves their colors. Green leaves receive their color from a green component called chlorophyll. The process of photosynthesis is aided by chlorophyll. It takes in sunlight's energy.

The leaves use the power to produce sugars, food for the plant. Understanding the variation within and between the crop's leaves

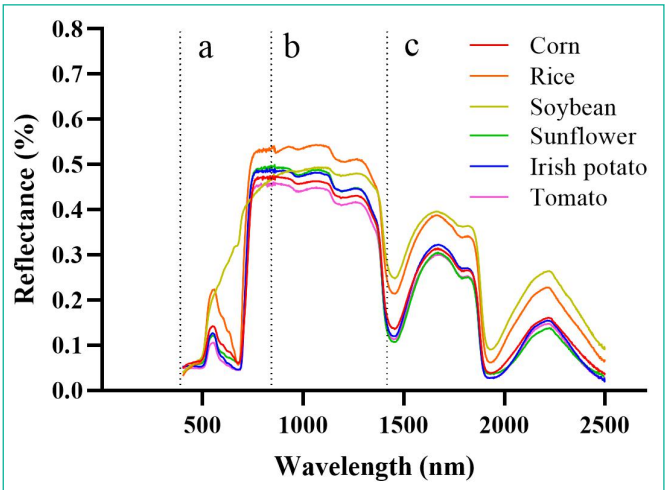

Figure 3: Spectral signatures pattern of the six major crops including cereal (Corn and rice) oil producing (soybean and sunflower), and vegetable (Irish potato and tomato).

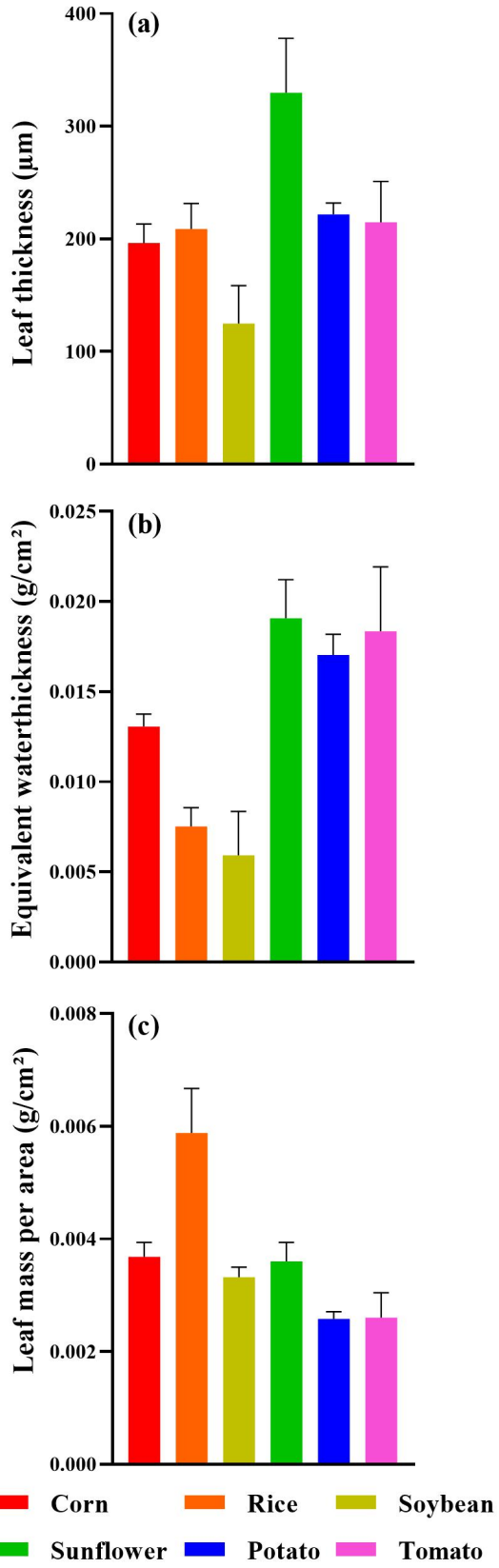

Figure 4: Representation of the average value and the standard deviation of the six sample crops leaves mass, equivalent water thickness, and leaf thickness.

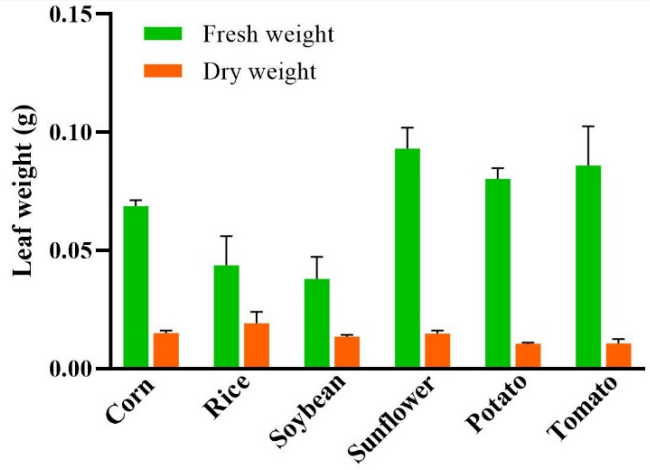

Figure 5: Representation of the fresh and dry leaf of six sample crops. Bar represent the average value of the sample leafs and lines represent the standard deviation of the sample weights.

could help to improve the relevant crop yield and save environmental resources. We have experimental data for six crops with five leaves samples for each crop [22,26]. The average thickness of the leave was found to be around 200 µm sunflower leave have a maximum value of 327 µm with higher variation. Vegetable crops have higher equivalent water thickness as compared to cereal crops. Rice leaf mass was observed at 0.0057 (g/cm2), which is greater than all other studied crops, while potato and tomato leaf mass was 0.0023 and 0.0024 (g/cm2) (Figure 4). Sample results showed a significant variation between the fresh leave weights and less variation between the dry weights of the studied crops. Vegetables leave have greater water content, so their fresh leave weight is higher than the other crops (Figure 5).

Many studies have used the solar spectral domain and the crop leaves physical information to estimate crop yield by developing the vegetation indices [16] and Gross Primary Production (GPP), canopy radiation use efficiency, crop coefficient, as well as crop nitrogen content, which was also investigated using the fluorescence signal, while the near-infrared domain was mainly used to detect crop water stress [27,33]. The retrieval of a secondary variable often requires the exploitation of different sources of information, which encompass the fusion of data provided by various sensors and over different spectral domains, as well as ancillary information related to the functioning of the soil-plant-atmosphere continuum, meteorological information or phenology [6,31].

Conclusion

Crop production, distribution, and marketing are all highly dependent on crop monitoring, and multispectral remote sensing is widely acknowledged as having significant promise for crop identification, area estimation, and condition assessment. Examining canopy reflectance measurements, Landsat data, and canopy radiation models during the past few years has led to a better knowledge of crops' spectral and biophysical characteristics. It has been observed that the spectrum pattern of the leaves of the different crops provides information connecting crop development. The temporal profile approach provides a conceptual framework consistent with crop growth characteristics, to which more spectral variables may be added when new sensors add more data. This document

makes recommendations for several particular study areas. One is integrating data and models of spectral reflectance with work on canopy structure and light absorption. Using a spectral estimate of LA1 and canopy light interception as inputs to crop development and yield models is one of the most promising remote sensing techniques; further study in this area is required. It is necessary to continue developing and improving crop radiation models by incorporating the effects of specular reflection and creating models for imperfect, nonhomogeneous crops. To empirically describe vegetation and advance canopy radiation transfer models, it is necessary to collect data sets that include leaf optical characteristics, canopy geometry, and canopies' bidirectional reflectance distribution functions. Non-nadir observations, high-resolution spectrometry, combined optical and microwave measurements, and polarization data to estimate specular reflection are other study topics with tremendous potential.

In conclusion, there have been considerable improvements in the technical ability to acquire and interpret multispectral data and in the scientific understanding of the spectral features of crops. Remote sensing applications can offer significant benefits in agricultural systems, including early crop stress detection, efficient resource management, improved yield forecasting, and optimized pesticide application. However, data availability, cloud cover, and expertise require attention. Overcoming these challenges can unlock the full potential of remote sensing in revolutionizing agriculture and promoting sustainable farming practices.

References

1. Aït Hssaïne Ali, Johannes B Ries, Klaus Daniel Peter, Irene Marzolff, and Sebastian d'Oleire-Oltmanns. Monitoring Soil Erosion in the Souss Basin, Morocco, with a Multiscale Object-Based Remote Sensing Approach Using UAV and Satellite Data. 2019: 562.
2. Allen WA, Richardson AJ. Interaction of Light with a Plant Canopy. Journal of the Optical Society of America. 1968; 58: 1023.
3. Alvarez-Vanhard E, Houet T, Mony C, Lecoq L, Corpetti T. Can UAVs Fill the Gap between in Situ Surveys and Satellites for Habitat Mapping?. Remote Sensing of Environment. 2020; 243: 111780.
4. Antoine R, T Lopez, M Tanguy, C Lissak, L Gailler, P Labazuy, et al. Geoscientists in the Sky: Unmanned Aerial Vehicles Responding to Geohazards. Springer Netherlands. 2020: 41.
5. Atkinson PM. Downscaling in Remote Sensing. International Journal of Applied Earth Observation and Geoinformation. 2013; 22: 106–14.
6. Barczewski, Stephanie. The Advantages of Using Drones over Space- Borne Imagery in the Mapping of Mangrove Forests. The American Historical Review. 2019; 124: 1522–23.
7. Bian, Jinhu, Ainong Li, Zhengjian Zhang, Wei Zhao, Guangbin Lei, and Haoming Xia. Grassland Fractional Vegetation Cover Monitoring Using The Composited Hj-1a / B Time Series Images And Unmanned Aerial Vehicles: A Case Study In Zoige Wetland, China 1. Institute of Mountain Hazards and Environment, Chinese Academy of Sciences, Cheng. Igarss. 2016; 2: 7192–95.
8. Brigot Guillaume, Elise Colin-Koeniguer, Aurelien Plyer, Fabrice Janez. Adaptation and Evaluation of an Optical Flow Method Applied to Coregistration of Forest Remote Sensing Images. IEEE Journal of Selected Topics in Applied Earth Observations and Remote Sensing. 2016; 9: 2923–39.
9. Briottet, Xavier, Rodolphe Marion, Veronique Carrere, Stephane Jacquemoud, Stephane Chevrel, Philippe Prastault, et al. HYPXIM: A New Hyperspectral Sensor Combining Science/Defence Applications. Workshop on Hyperspectral Image and Signal Processing, Evolution in Remote Sensing. 2011; 3: 10019.
10. Cândido, Anny Keli Aparecida Alves, Antonio Conceição Paranhos Filho, Marcelo Ricardo Haupenthal, Normandes Matos da Silva, Jonas de Sousa Correa, et al. Water Quality and Chlorophyll Measurement Through Vegetation Indices Generated from Orbital and Suborbital Images. Water, Air, and Soil Pollution. 2016; 227: 224.
11. Carbonneau PE, Belletti B, Micotti M, Lastoria B, Casaioli M, Mariani S, et al. UAV-Based Training for Fully Fuzzy Classification of Sentinel-2 Fluvial Scenes. Earth Surface Processes and Landforms. 2020; 45: 3120–40.
12. Casagli, Nicola, William Frodella, Stefano Morelli, Veronica Tofani, Andrea Ciampalini, Emanuele Intrieri, et al. Spaceborne, UAV and Ground-Based Remote Sensing Techniques for Landslide Mapping, Monitoring and Early Warning. Geoenvironmental Disasters. 2017; 4: 1–23.
13. Colomina I, Molina P. Unmanned Aerial Systems for Photogrammetry and Remote Sensing: A Review. ISPRS Journal of Photogrammetry and Remote Sensing. 2014; 92: 79–97.
14. Fourty TH, Baret F. On Spectral Estimates of Fresh Leaf Biochemistry." International Journal of Remote Sensing. 1998; 19: 1283–97.
15. Jacquemoud S, Ustin SL, Verdebout J, Schmuck G, Andreoli G, Hosgood B. Estimating Leaf Biochemistry Using the PROSPECT Leaf Optical Properties Model. Remote Sensing of Environment. 1996; 56: 194–202.
16. Liu Peng, Liping Di, Qian Du, Lizhe Wang. Remote Sensing Big Data: Theory, Methods and Applications. Remote Sensing. 2018; 10: 711.
17. Marx A, McFarlane D, Alzahrani A. UAV Data for Multi-Temporal Landsat Analysis of Historic Reforestation: A Case Study in Costa Rica. International Journal of Remote Sensing. 2017; 38: 2331–48.
18. Melesse AM, Weng Q, Thenkabail PS, Senay GB. Remote Sensing Sensors and Applications in Environmental Resources Mapping and Modelling. Sensors. 2007: 3209–41.
19. Melville B, Fisher A, Lucieer A. Ultra-High Spatial Resolution Fractional Vegetation Cover from Unmanned Aerial Multispectral Imagery. International Journal of Applied Earth Observation and Geoinformation. 2019; 78: 14–24.
20. Müllerová Jana, Josef Brůna, Tomáš Bartaloš, Petr Dvořák, Michaela Vítková, Petr Pyšek. Timing Is Important: Unmanned Aircraft vs. Satellite Imagery in Plant Invasion Monitoring. Frontiers in Plant Science. 2017; 8: 887.
21. Müllerová Jana, Josef Brůna, Petr Dvořák, Tomáš Bartaloš, Michaela Vítková. Does the Data Resolution/Origin Matter? Satellite, Airborne and UAV Imagery to Tackle Plant Invasions. International Archives of the Photogrammetry, Remote Sensing and Spatial Information Sciences - ISPRS Archives. 2016; 41: 903–8.
22. Naveed, He HS, Zong S, Du H, Satti Z, Sun H, et al. Cotton Cultivated Area Detection and Yield Monitoring Combining Remote Sensing with Field Data in Lower Indus River Basin, Pakistan. Environmental Monitoring and Assessment. 2023: 195.
23. Naveed M, He H, Zong S, Du H, Satti Z, Tan X, et al. Spatial Pattern of Cotton Yield Variability and Its Response to Climate Change in Cotton Belt of Pakistan. Chinese Geographical Science. 2023; 33: 351–62.
24. Papakonstantinou A, Doukari M, Stamatis P, Topouzelis K. Coastal Management Using UAS and High-Resolution Satellite Images for Touristic Areas. International Journal of Applied Geospatial Research. 2019; 10: 54–72.
25. Phiri Darius, Matamyo Simwanda, Serajis Salekin, Vincent Raphael Nyirenda, Yuuji Murayama. Sentinel-2 Data for Land Cover / Use Mapping: A Review Sentinel-2 Data for Land Cover / Use Mapping: A Review. 2020.
26. Pohl C, JL Van Genderen. Review Article Multisensor Image Fusion in Remote Sensing: Concepts, Methods and Applications. 1998: 19.
27. Riihimäki H, Luoto M, Heiskanen J. Estimating Fractional Cover of Tundra Vegetation at Multiple Scales Using Unmanned Aerial Systems and Optical Satellite Data. Remote Sensing of Environment. 2019; 224: 119–32.
28. Rupasinghe PA, Milas AS, Arend K, Simonson MA, Mayer C, Mackey S. Classification of Shoreline Vegetation in the Western Basin of Lake Erie Using Airborne Hyperspectral Imager HSI2, Pleiades and UAV Data. International Journal of Remote Sensing. 2019; 40: 3008–28.

29. Saeed Sadaf, Ri Liu, Mingyan Gao, Dongdong Liu, Zuobin Wang, Ali Zia. Hierarchical and Gradient Si Nano Wires-Holes Arrays by LIL and MACE. 2022 IEEE International Conference on Manipulation, Manufacturing and Measurement on the Nanoscale, 3M-NANO 2022 - Proceedings (August). 2022: 568–71.

30. Sarvia, Filippo, Elena Xausa, Samuele De Petris, Gianluca Cantamessa, Enrico Borgogno-mondino. A Possible Role of Copernicus Sentinel-2 Data to Support Common Agricultural Policy Controls in Agriculture. 2021: 1–19.

31. Solazzo D, Sankey JB, Ts Sankey T, Munson SM. Mapping and Measuring Aeolian Sand Dunes with Photogrammetry and LiDAR from Unmanned Aerial Vehicles (UAV) and Multispectral Satellite Imagery on the Paria Plateau, AZ, USA. Geomorphology. 2018; 319: 174–85.

32. Sun AY, Scanlon BR. How Can Big Data and Machine Learning Benefit Environment and Water Management: A Survey of Methods, Applications, and Future Directions. Environmental Research Letters. 2019: 14.

33. Wang R, Zhang S, Pu L, Yang J, Yang C, Chen J, et al. Gully Erosion Mapping and Monitoring at Multiple Scales Based on Multi-Source Remote Sensing Data of the Sancha River Catchment, Northeast China. ISPRS International Journal of Geo-Information. 2016: 5.

34. Wulder MA, White JC, Loveland TR, Woodcock CE, Belward AS, Cohen WB, et al.. The Global Landsat Archive: Status, Consolidation, and Direction. Remote Sensing of Environment. 2016; 185: 271–83.

35. Xia H, Wei Z, Li A, Bian J, Zhang Z. Subpixel Inundation Mapping Using Landsat-8 OLI and UAV Data for a Wetland Region on the Zoige Plateau, China. Remote Sensing. 2017; 9: 1–22.

36. Yasir QM, Zhang Z, Tang J, Naveed M, Jahangir Z. Spectral Indices for Tracing Leaf Water Status with Hyperspectral Reflectance Data. 2023; 17: 1–19.

37. Zhang J. Multi-Source Remote Sensing Data Fusion: Status and Trends. International Journal of Image and Data Fusion. 2010; 1: 5–24.

38. Zhu X, Cai F, Tian J, Kay-Ann Williams T. Spatiotemporal Fusion of Multisource Remote Sensing Data: Literature Survey, Taxonomy, Principles, Applications, and Future Directions. Remote Sensing. 2018: 10.